Object-based, multi-sensor habitat mapping of successional age classes during a 70-year secondary forest succession

Sawaid Abbas [a] • Janet E. Nichol [a] • Man Sing Wong [a b] *

[a] Department of Land Surveying and Geo-Informatics, the Hong Kong Polytechnic University, Hong Kong

[b] Research Institute for Sustainable Urban Development, the Hong Kong Polytechnic University, Hong Kong

emails: sawaid.abbas@gmail.com (**S.Abbas**), lsjanet@polyu.edu.hk (**J. E. Nichol**), ls.charles@polyu.edu.hk (**M. S. Wong**).

Tel.: +1-852-3400-8959; Fax: +1-852-2330-2994

* Corresponding Author

Object-based, multi-sensor habitat mapping of successional age classes for effective management of a 70-year secondary forest succession

Abstract: Multi-temporal change detection over decades including the pre-satellite era is challenging due to the different image types available over time, and this explains the scarcity of long-term studies of vegetation succession which can play a pivotal role in the restoration of biodiversity in regenerating forests. This study describes a semi-automated, object-based habitat classification method for change detection of tropical forest succession since 1945. The study uses a set of black and white aerial photographs and high-resolution satellite images which differ in quality and resolution, to investigate forest successional patterns and their implications for informed ecosystem and land rehabilitation management. For optimized habitat boundary delineation from black and white aerial photographs and panchromatic satellite images, three levels of hierarchical image object primitives were created. The minimum object sizes of 50 m^2, 500 m^2, and 1000 m^2 maximized inter-object and minimized intra-object variability according to the scale of habitat patches and imagery used. Object-Based Image Analysis (OBIA) provided additional Grey-Level Co-occurrence Matrix (GLCM) textural features of segmented objects which helped to incorporate knowledge-based rule-sets into the final habitat classification which was done manually by an experienced interpreter. Results show accuracies for grassland greater than 94 %, monoculture plantations were distinguished from natural forest with 95 % accuracy, and isolated mature stands of natural forest achieved 75 % accuracy. Consideration of multi-date images increased the accuracy of distinguishing between mixed plantations and natural forest as well as between shrubland and young secondary forest. The resulting maps of vegetation structure at five time periods from 1945 to present gave new insights into the ecological processes of secondary forest succession. These include the surprising rapid rate of natural forest regeneration, at an annual rate of 7.7 %

from 1945 to 2014, and an even faster rate of 11 % during a period when hill fires were controlled. The last areas to succeed to forest are those which are still, or at some time have been under exotic mono-cultural plantations. This suggests that long term protection from hill fire would be a better option for assisting natural succession in the landscape than plantations, which are both costly, and act as barriers to natural succession. Overall, with more than 92% mapping accuracy, the method can be adapted for other multi-temporal, multi-sensor studies as it enables inclusion of spatial theories by dividing the satellite image into time-consistent geographic entities according to the scale of target objects and image resolution. The accurate maps of forest cover patches at different successional stages can also help in site specific management of the recovering forest, such as introduction of shrub seedlings to bridge bottlenecks in seed dispersal according to shrub density and dispersal distances for forest birds. Late successional tree species can also be introduced in areas where only early successional species are present after 50 years of succession.

Key Words: temporal mapping; forest succession; aerial photograph; Hong Kong

1. Introduction

Deforestation is occurring at an alarming rate in tropical forests and therefore is one of the primary threats to biodiversity (Sodhi and Brook, 2008; Turner and Corlett, 1996). Despite the large scale exploitation of these tropical resources, a few small areas, such as in Brazil (Kim et al., 2015; Perz and Skole, 2003) Puerto Rico (Grainger, 1988), Costa Rica (Hartshorn, 1980; Helmer, 2000), Mexico (Guevara and Laborde, 1993), Colombia (Faber-Langendoen, 1992), Venezuela (Saldarriaga et al., 1988), Myanmar (Sann et al., 2016), Singapore (Turner et al., 1997) and Hong Kong, have been given chance to regrow as a result of natural regeneration or large scale afforestation programs (Grainger, 1988; Perz and Skole, 2003). Although many governments expend large resources on afforestation projects, natural succession may be equally effective if informative data on rates and pathways of secondary forest succession can be provided. Knowledge of recovery rates, variation in regrowth rates across time and space, and the responses of post-disturbance regeneration of tropical forest to environmental gradients are vital to facilitate biodiversity conservation and management of these recovering ecosystems.

Remote sensing provides an indispensable source of information for observing spatial and temporal patterns of forest ecosystems and conservation planning. However, satellite remote sensing-based mapping of spatial and temporal patterns of forest cover change is temporally limited from 1972 to present, while utilizing the data of the long running Landsat earth observation program (Vogeler et al., 2018). But, longer time series analysis (e.g., more than 70-years) of habitat mapping of successional age classes of recovering tropical forest is vital for effective management of secondary forest succession. In addition to limited temporal range, these data sets are relatively coarse in spatial resolution (~ 80 m to 30 m) which might not be sufficient for fine scale characterization of pathways and spatio-temporal patterns of recovering tropical forest.

On the other hand, black and white aerial photographs provide the earliest temporal record of remote sensing data and therefore are invaluable sources for studies of change in ecosystem dynamics over time (Allard, 2003; Dissanska et al., 2009; Pellerin and Lavoie, 2003; Pringle et al., 2009; Rabia and Terribile, 2013). It has been widely used by ecologists for fine scale mapping of tropical forest to assist conservation planning and management (Etter et al., 2005; Galo, 2016; Turner et al., 1996). However, multi-temporal change detection from aerial photographs over the past decades including the pre-satellite era (i.e. before 1970s) is still challenging due to the different image types available over time, and this explains the scarcity of long-term studies of vegetation succession which can play a pivotal role in the restoration of biodiversity in regenerating forest.

Nonetheless, delineation of habitat patches from high-resolution remote sensing data is difficult, especially when consistency among different image types is required. The tonal and structural complexity of habitat patches exhibit differently between black and white aerial photographs and multispectral satellite images. The image interpretation requires theories and methods to identify, and abilities to link the landscape components or objects at their respective scales, within hierarchical mapping structures (Hay et al., 2003). Moreover, these structures must be consistent over time, even as the landscape is changing over multiple mapping periods. However, how the spatial patterns in the landscape change over time depends on the scale of observation, and this invokes the modifiable areal unit problem (MAUP) (Marceau et al., 1994), because mapped units merging or separating may form a different class according to their scale. This problem is compounded when using multi-source data of differing scales and resolutions. Therefore, considering, the subjectivity of determining the boundary between the habitat classes, and the different types and scales of imagery used, a multiscale object-based paradigm of habitat delineation is required to segment the image into multiple object primitives according to both spatial and spectral characteristics.

As in many developed countries, Hong Kong's natural vegetation is confined to steeply sloping mountainous areas, and 40% of Hong Kong's land area is reserved in Country Parks, where natural regeneration is evident. These changing patterns of landscape, with vegetation succession from open ground to forest, are indicative of changing ecological processes operating along the successional gradient, and can be informative for devising realistic conservation policies. The situation of recovering secondary forest in Hong Kong, coupled with post World War II aerial photographs since 1945, and recent high-resolution satellite imagery, provides an opportunity to monitor and assess natural structural succession of regenerating vegetation. Each structural stage exhibits different canopy structures and stand heights that produce distinctive tone and texture on aerial photographs and satellite images (Geri et al., 2010; Munsi et al., 2010; Song and Woodcock, 2002; Teferi et al., 2013). Therefore, succession in structural stages can be mapped visually using high resolution historic aerial photographs and recent satellite images (Lucas et al., 2002; Qi et al., 2013).

In this study, a semi-automated, object-based habitat classification methodology was used for change detection using a set of black and white aerial photographs and high-resolution panchromatic satellite images with different qualities and resolutions. The aim is to investigate vegetation successional patterns and their implications for forest restoration and biodiversity conservation. The study developed a methodology for change detection of a 70-year secondary forest succession using multi-sensor images. Additionally, the results would suggest how the findings may be used to inform restoration of landscapes degraded following shifting cultivation, which is widespread in the Asian sub-tropics.

2. Study Area

Hong Kong is a special administrative region of Mainland China, is situated between 22 º 09 □ to 23 º 37 □ latitudes and 113º52□ to 114º30□ longitudes on the northern margins of the Asian tropics (Figure 1). The study area extends over ~2800 ha comprising the Tai Mo Shan

and Shing Mun country parks in the New Territories of Hong Kong (Figure 1). The topography is rugged, characterized by convex slopes rising to Hong Kong's tallest peak Tai Mo Shan (957 m), and steep-sided slopes around Shing Mun reservoir.

The climate of Hong Kong includes features of both the tropics and subtropics with highly seasonal rainfall and temperature. Despite being located 100 km south of the Tropic of Cancer, the climate is best described as subtropical due to temperature and rainfall seasonality with a hot humid summer from May to September and a cool dry winter from November to February (Leung et al., 2008).

Hong Kong is an ideal study area to ascertain spatial patterns of structural changes during secondary forest succession, due to a combination of well-documented flora, a complex mixture of environmental gradients, easy access to field sites, recovering secondary forest since 1945, and availability of historical archived aerial photographs.

2.1 Description of vegetation in the study area

Current forest cover in Hong Kong comprises Feng Shui Woods (Zhuang and Corlett, 1997), natural secondary forest, and plantations. Upper valleys are covered with fire-maintained grasses and lower elevations support patches of secondary forest and plantations (Delang and Hang, 2009). Hong Kong's primeval vegetation was a diverse seasonal rain forest with at least 150-180 woody species per hectare, as found in nearby protected areas in South China (Cao et al., 2013; Jingyun et al., 2004). Subsequently, following centuries of terrace agriculture, deforestation in WW2 and degradation to fire-maintained grasslands, natural forest succession is now occurring, and the process is said to be very slow (Dudgeon and Corlett, 2011). Thus, the majority of the secondary forest has developed through structural succession on lands protected from fire since 1945. The early successional forests in the study area are mosaics of shrubs and trees. Species richness in a 400 m^2 forest plot ranges from 19 to 61 depending upon

age and location of forest patches in the study area (unpublished data). Most of the climax trees are absent from the secondary forests and are mostly restricted to very small pockets of remnant forests along streams and better protected places near villages. At lower elevations (< 500 m), natural invasion starts from light-demanding pioneers, such as *Aporosa octandra, Sterculia lanceolate, Acronychia pedunculata, Daphniphyllum calycinum, Schefflera heptaphylla, Sapium discolor, Diospyros morrisiana*, *Ficus variolosa*, *Psychotria asiatica*, and *Ardisia quinquegona*, to the large dominant species in older sites (> 70 year old) such as, *Sarcosperma laurinum, Bischofia jananica, Cryptocarya chinensis, Elaeocarpus chinensis,* and *Choerospondias axillaris.* Whereas grassland in the higher elevations (> 500 m) are first colonized with species such as, *Machilus chekiangensis, Gordonia axillaris, Melastoma malabathricum,* and *Eurya chinensis,* and later dominated by species such, as *Myrsine seguinii, Machilus breviflora, Ilex viridis, Camellia caudata, Symplocos sumuntia, and Ligustrum japonicum*.

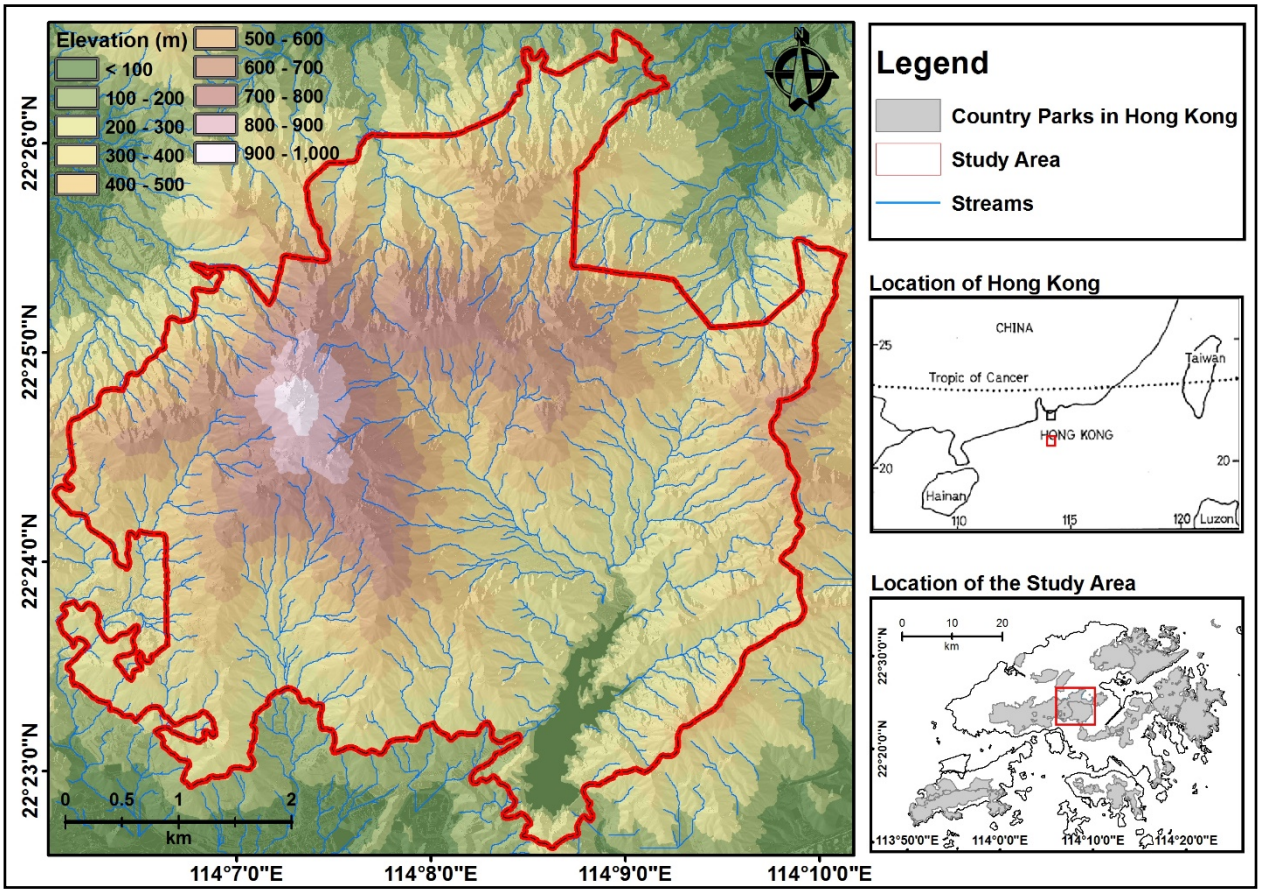

Figure 1 Location map of the study area

3. Material and Methods

3.1 Data acquisition and pre-processing

Remote sensing data used for this study consisted of three subsets of archived aerial photographs since 1945 and two satellite images. Complete coverage of Hong Kong is available since 1945. Black and white aerial photographs of 1945 (scale - 1:40,000), 1963 (scale - 1:14,000) and 1989 (scale - 1:20,000) of the study area were obtained from the Lands Department of Hong Kong (HK-LandsD, 2014) and VHRS (Very High-Resolution Satellite) cloud free panchromatic images for years 2001 (IKONOS – spatial resolution of 1 m) and 2014 (World View 2 - spatial resolution of 0.5 m) were procured from Digital Globe. The panchromatic satellite images were used, instead of pan-sharpened or multispectral images, in

order to ensure consistency of methods with black and white aerial photographs. In addition, a very high resolution (2 m spatial resolution) Digital Elevation Model (DEM) and a digital orthophoto (0.5 m spatial resolution) were obtained from the Lands Department of Hong Kong.

In total 43 photos (18 for 1945, 12 for 1963 and 13 for 1989) were scanned at resolution of 1200 dpi and ortho-rectification was done using 15 to 20 well distributed GCPs (Ground Control Points) for each photo. The X and Y coordinates of the GCPs were collected from the digital orthophoto and Z values were taken from the DEM. After geometric correction, the individual orthophotos were clipped and mosaiced to form unified images. The satellite images were also ortho-rectified using the RPC (Rational Polynomial Coefficients) along with the ortho-photo and the DEM. Later, all data sets were re-projected into Hong Kong's local projection system, the Hong Kong 1980 Grid system. For consistency, all the data sets were co-registered with the digital orthophoto with an RMSE (Root Mean Square Error) ranging from less than 1, to 5 m, depending on the scale and resolution of the datasets. For subsequent analysis, all data sets were resampled to a common pixel size (0.5 m) and radiometric level (8-bit grey scale).

3.2 Habitat Classes

Prior knowledge and description of habitat classes is critical for precise and reliable mapping. An 'a priori' habitat classification scheme was derived from previous habitat mapping in Hong Kong (Ashworth et al., 1993) as it was based on vegetation structural characteristics observable on remotely sensed images (Table 1). Descriptive information of the classification scheme was based on a standardized classification scheme of the Land Cover Classification System (LCCS) (Congalton et al., 2014).

Table 1 Description of habitat classes

Class Name	Description of class
Forest (F)	Tree Cover, broadleaved, evergreen, close to open (canopy > 60-70%)
Open Forest (OF)	Mosaic: Tree Cover, broadleaved, evergreen, open canopy (15 - 60 %) and Shrubland and / or Grassland
Shrubland (SH)	Shrubland, broadleaved, evergreen, close, canopy > 60 - 70 %
Open Shrubland (SG)	Mosaic: Shrubland, broadleaved, evergreen, open canopy > 15 - 60 % and Grassland
Grassland (GL)	Ground story grasses as dominant vegetation form
Plantation Forest (PF)	Primarily monoculture stands plantation forest -*Melaleuca quinquenervia*, *Lophostemon confertus, Acacia confusa,* and few mixed plantation patches
Bare Areas (BA)	Areas without significant vegetation forms; consists of exposed soil / rocks / tracks
Built up Area (BU)	Manmade features
Water (W)	Natural / Manmade water bodies

3.3 Segmentation and habitat classification

Habitat patches occur at a variety of spatial and temporal scales and are dynamic in nature. A patch at any scale includes patchiness at finer scale which represents the internal structure of the patch and a mosaic is defined by patchiness at broader scale. Therefore, in this study, a multiscale object-based paradigm was adopted to accommodate different original scales and resolution of imagery used, as well as the subjectivity of determining boundaries among

196 different habitat classes. The foremost part of Object-Based Image Analysis (OBIA) is a
197 segmentation of an image into multi-pixel image object primitives. During this process, an
198 image object level is created, or the morphologies of already existing objects are altered. The
199 result of segmentation is controlled by user-defined scale parameters which must be selected
200 according to the size and features of expected objects (Mathieu et al., 2007). The scale
201 parameter is directly related to the average size of the objects being detected. Its function of
202 spectral heterogeneity which is defined as the weighted sum of standard deviations of the
203 spectral values in each image layer. The larger the scale factor, the higher the allowed
204 heterogeneity, and the greater will be the size of objects and vice versa. For the current image
205 analysis, the scale parameters were defined by a trial and error approach in order to acquire
206 optimum image objects of interest. The defined objects maximize inter-object and minimize
207 intra-object variability according to the specified spatial scale of the objects (Flanders et al.,
208 2003). Thus, the segmentation process can be seen as an automated digitizing of habitat
209 boundaries. In particular, it is a more standardized method than manual digitizing of habitat
210 patches, when airborne photographs need to be compared to high-resolution satellite images.
211 Thus, the semi-automated object-based approach combines texture and tonal characteristics of
212 image object primitives which may be less constrained by the imagery used.

213 The multi-resolution segmentation resulted in three levels of hierarchical image object
214 primitives with minimum object sizes of 50 m^2, 500 m^2, and 1000 m^2 (Table 2). Segmentation
215 of the image data at fine and coarse scales was important to extract boundaries of the
216 representative habitat objects occurring at their corresponding scales, as due to the Modifiable
217 Areal Unit Problem (MAUP), pixels belonging to small or large patches may be classified
218 differently simply according to the patch size. For example, upper level segments were used
219 for large patches of grassland, forest and monoculture plantation stands. The difference
220 between two ecologically meaningful classes ‘shrubland’ and ‘open shrubland’, or between

two classes ‘forest’ and ‘open forest’ is dependent on the mapping scale. At finer scale, small isolated patches of ‘forest’ and ‘shrubland’ could be defined, while the less stringent homogeneity required for medium scale patch definition was able to identify ‘open forest’ and ‘open shrubland’. These are important successional classes for understanding the natural transition from open grassland to closed forest, which starts with isolated patches of shrub, whose seeds are distributed into grassland by forest birds flying between forest patches. Contiguous regions of similar class were merged together to form continuous patches.

The next step of interpreting and classifying was done subjectively by an experienced interpreter, and was based on tone, texture, and habitat association of image object primitives. A gradient of black to grey tone, rough to smooth texture, large to small crown size, and long to short shadow, was used to recognize forest, open forest, shrubland, open shrubland and grassland. Three grey level co-occurrence matrix (GLCM) based textural features (Haralick et al., 1973), namely GLCM homogeneity (*H*), GLCM contrast (*C*) and GLCM standard deviation (SD) of all directions, were also used to assist the process of habitat classification of image object primitives. GLCM contrast (*C*) measures the amount of local variations of intensity between a pixel and its neighboring pixels in an object (equation I), homogeneity (*H*) estimates the closeness of the distribution of elements in GLCM which decreases exponentially if an object is heterogeneous and values of elements are not concentrated along the diagonal of GLCM (equation II), and standard deviation (S) measures the dispersion of values around the mean (equation III). The three GLCM textural properties are defined in equations I and II (Hall-Beyer, 2007). After classification, all the habitat maps were converted to raster grids of 1 m.

$$C = \sum_{i,j=0}^{N-1} P_{i,j}(i-j)^2 \quad \text{(I)}$$

$$H = \sum_{i,j=0}^{N-1} \frac{P_{i,j}}{1+(i-j)^2} \quad \text{(II)}$$

$$S = \sqrt{\sum_{i,j=0}^{N-1} P_{i,j}\,(i,j - \mu_{i,j})} \quad \text{(III)}$$

where $P_{i,j}$ is a normalized co-occurrence matrix, i and j are number of rows and column, and N is the dimension of the matrix.

Table 2 Segmentation parameters used for three levels of the segmentation based on trial and error approach

Year of Image	1945	1963	1989	2001	2014	MMU (m2)	Target Class
Image Scale / Resolution	1:40K	1:14K	1:20K	1 m	0.5 m		
Segmentation Parameters	Shape = 0.3, Compactness = 0.5						
Level 1 - Scale	100	140	125	140	145	1000	Large Patches of Forest, Grasses, and Plantations
Level 2 - Scale	40	65	50	60	70	500	Open Forest, Open Shrubland, and Shrubland
Level 3 - Scale	20	30	22	28	25	50	Isolated Shrubs, and Open Forest

3.4 Field Data Collection

Training areas and ground truth information were obtained from the comprehensive *in-situ* data from a previous habitat mapping study in the study area, in the form of 352 field surveyed GPS points and 215 additional check points on very high-resolution color aerial photographs (Nichol and Wong, 2008). In addition, a floristic survey of vegetation was conducted between March 2015 and May 2016. Vegetation census data were collected by establishing 28 quadrats (20 m x 20 m) distributed along the elevation gradient and by considering the age of forest stands in the study area (figure 4). The minimum age of forest patches was determined from the five habitat maps (figure 4). Considering the heterogeneity in the landscape and accessibility, it was difficult to find continuous vegetation cover with similar types through random selection, therefore, stratified random sampling was used to select 28 plot locations. The sites were selected to maximize the range of vegetation types sampled and to occupy the geographic

extent of the study area. Plots were located in different forest patches of the five vegetation communities (forest since 1945, forest since 1963, forest since 1989, forest since 2001, and forest since 2014). It was attempted to sample each vegetation community at an altitudinal interval of 200 m, and further divided into cardinal slope directions (N, NE, E, SE, S, SW, W, and NW), as well as slope (flat, gentle, moderate, and steep), whenever possible.

3.5 Accuracy assessment

A 'K x K' confusion matrix was generated to determine the degree of error in the maps by calculating the producer's accuracy, user's accuracy and kappa statistics (Lillesand et al., 2004). Accuracy assessment of the habitat mapping of 2001 was performed using the ground reference points collected during the previous mapping activities in the study area, by Nichol & Wong (2008) while habitat mapping of 2014 was examined using field data collected from several field surveys conducted between March 2015 and May 2016.

3.6 Annual rate of change and transitions among habitat classes

Maps were sequentially paired (1945-1963, 1963-1989, 1989-2001, and 2001-2014) and the change matrices were produced from the five habitat maps, by overlapping and cross tabulation of two habitat maps of the successive time periods. To summarize the transition, further analyses were carried out to determine gain (equation IV), loss (equation V), net change (equation VI), swap (equation VII), and total change (equation VIII) in each structural class for each of the periods (Pontius et al., 2004). The annual rates of change in habitat classes were computed using equation IX (Puyravaud, 2003; Teferi et al., 2013).

$$G_j = P_{+j} - P_{jj} \qquad \text{Equation (IV)}$$

$$L_j = P_{j+} - P_{jj} \qquad \text{Equation (V)}$$

$$(ANc)_j = |P_{+j} - P_{j+}| \qquad \text{Equation (VI)}$$

$$S_j = 2\min\left(P_{j+} - P_{jj}\,;\, P_{+j} - P_{jj}\right) \quad \text{Equation (VII)}$$

$$(Tc)_j = \left(P_{j+} - P_{jj}\right) + \left(P_{+j} - P_{jj}\right) \quad \text{Equation (VIII)}$$

$$R = \left(\frac{1}{T_2 - T_1}\right) \times \left(\ln \frac{A_2}{A_1}\right) \times 100 \quad \text{Equation (IX)}$$

where R is the rate of change (% per year), A_1 and A_2 represent area corresponding to earlier time, T_1, and later time, T_2. Gain (G) refers to the percentage of a habitat category in the later landscape after subtracting its proportion in the earlier landscape, and the Loss (L) was the difference between percentage of a category in the earlier landscape and its proportion that persisted in the landscape over a transition period. Absolute Net Change (ANc) was the absolute difference of proportion of a category in the earlier and the later landscape. Swap (S) represents the amount of a habitat category lost at one location while the same amount is added at a different site in the landscape. The total change (Tc) was calculated to conclude the overall change in a category by summing up the G and L.

4. Results

4.1 Segmentation and classification

A combination of tonal and textural parameters in OBIA allowed ruled based extraction of most habitat features. Grasslands were easily distinguished through high homogeneity (0.90 to 0.92) and low internal contrast (1.56 to 5.92). Although plantation and forest objects had overlapping ranges of contrast and homogeneity, 95 % of the plantation patches were distinguishable from natural forest stands by using the error range ((mean (μ) ± standard deviation (σ))) of the GLCM features - homogeneity (H) and standard deviation (Table 3). Forest, open forest, shrubland and open shrubland were similar on the homogeneity spectrum with overlapping ranges of standard deviation and contrast. Out of these habitat classes, only mature forest stands with varying crown size and elongated shadows could be successfully separated using a combination of standard deviation (28.23 – 45.07) and homogeneity (0.64 to 0.72). GLCM-based rule sets helped to classify more than 94 % of grassland objects (94% accuracy), to distinguish 95 % of monoculture plantation objects from natural forest (95 %

312 accuracy), and isolated mature of stands of natural forest achieved 75 % accuracy. It was
313 difficult to define rules to distinguish between open forest, shrubland and open shrubland due
314 to overlapping ranges of the GLCM parameters and therefore these were manually classified.
315 In addition, image segments comprising two or more habitat classes, for example, an object
316 encompassing open forest and open shrubland, were classified at finer scale segments at second
317 and third levels of segmentation. Overall, the object-based framework was very useful first for
318 automatic delineation of habitat boundaries using multi-resolution image segmentation and
319 then by applying rule sets to classify more than 50 % of the created objects into corresponding
320 habitat classes, while the remaining unclassified objects were classified using other criteria
321 such as temporal change and visual interpretation.

322 **Table 3** GLCM textural characteristics of vegetation structural classes (mean (μ) ± standard
323 deviation (σ))

	Standard Deviation (SD)	Contrast (C)	Homogeneity (H)
Forest	36.65 ± 8.42	49.70 ± 23.10	0.69 ± 0.04
Open Forest	16.78 ± 4.02	21.42 ± 19.47	0.80 ± 0.01
Shrubland	24.43 ± 1.54	13.18 ± 3.11	0.73 ± 0.02
Open Shrubland	19.13 ± 4.91	16.46 ± 8.05	0.79 ± 0.02
Grassland	16.14 ± 2.82	3.74 ± 2.18	0.91 ± 0.01
Plantation	14.10 ± 1.14	28.96 ± 1.47	0.63 ± 0.01

324

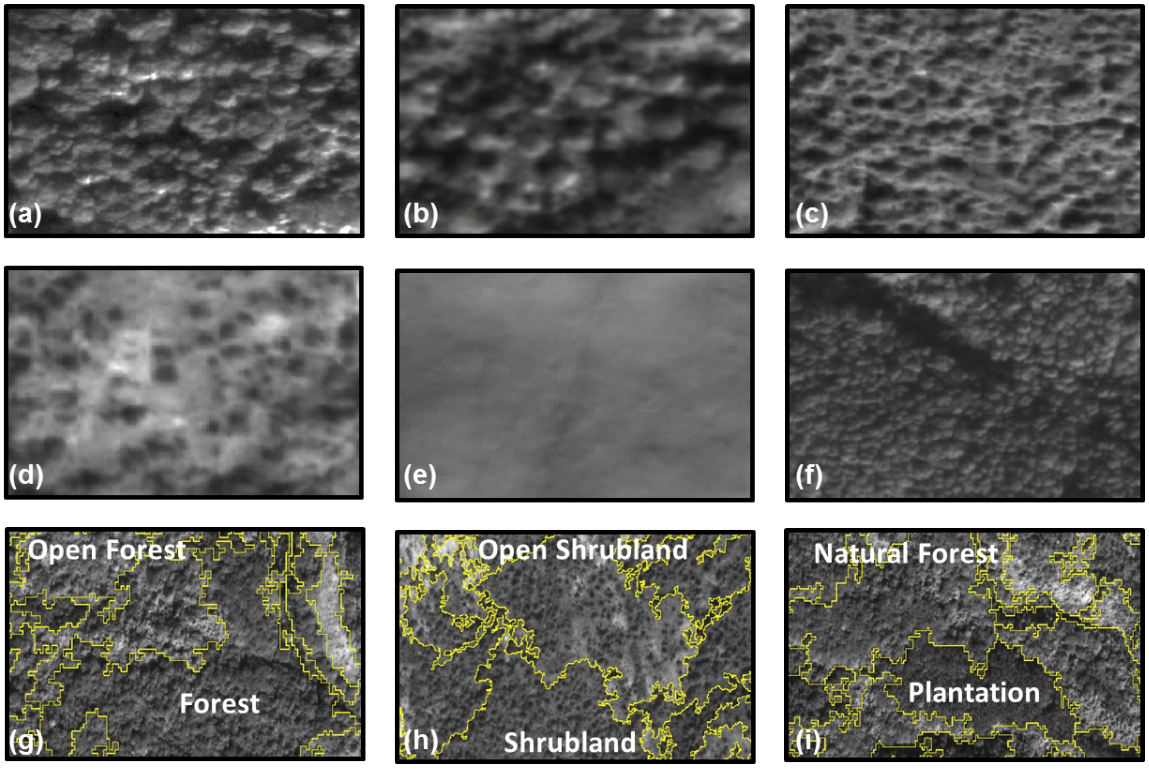

Figure 2 – Habitat classification legend (a) Forest - larger crown, longer shadows, higher density (b) Open Forest - larger crown, longer shadows, lower density (c) Shrubland - smaller crown, shorter shadows, higher density (d) Open Shrubland - smaller crown, shorter shadows, lower density (e) Grassland – smooth texture (f) Plantation – even canopy, homogenous tonal pattern (g) Segment boundaries between Open Forest and Forest (h) Segment boundaries between Shrubland and Open Shrubland (i) Segment boundaries between natural Forest and Plantation

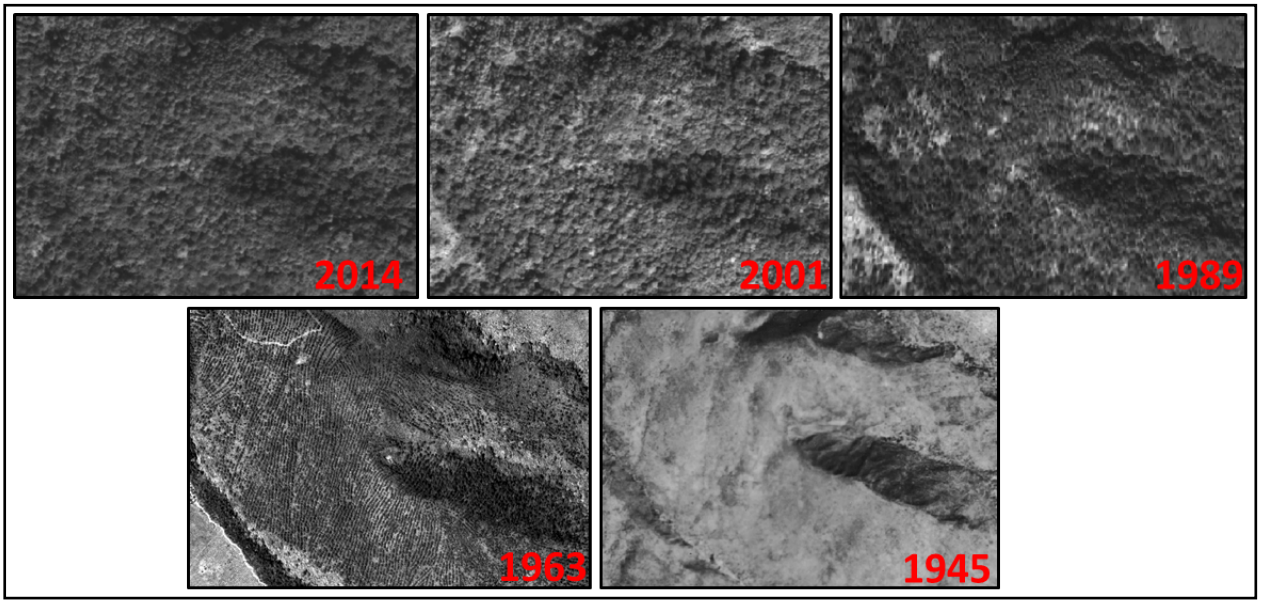

Figure 3 Plantation patches at their earlier growth stage, recognizable from their spatial pattern and arrangement in 1963

337 ## 4.2 Multi-temporal habitat Mapping

338 Five habitat maps were produced for the years 1945, 1963, 1989, 2001 and 2014 using the
339 multiscale object-based classification (Figure 4) and consecutive habitat maps were overlaid to
340 observe systematic transitions among structural classes while classifying the segmented
341 objects. The need to consider temporal change as part of the classification process because
342 change over time assisted identification meant that the method could not be completely
343 automated. Thus, observation at multiple time steps substantially improved the mapping, as the
344 successional stages tend to proceed logically. For example, if an image segment classified as
345 forest or open forest at a later time was not shrubland or open shrubland at an earlier time and
346 there was no strong evidence to classify the patch as forest (such as long shadows and bigger
347 crown), then the patch was assigned to shrubland (if the density was high) or open shrubland
348 (if the density was low). Additionally, since it was difficult to distinguish between plantations
349 and natural forest at a mature stage, going back to a time when plantations were young or at an
350 early stage, and identifiable from the regular planting pattern, helped to confirm the segments
351 as plantation. In this regard, aerial photographs of 1963 had significant value, as most large-
352 scale plantation stands of native species (needle-leaved *Pinus massoniana*) and mixed species
353 were planted between 1945 and the early 1970s (Figure 3). On the other hand, monoculture
354 stands of exotic species (Figure 2) planted since the late 1970s were easily recognizable
355 through their homogenous pattern even at a mature stage. Thus overall, high mapping
356 accuracies were achieved by application of the three steps (i) multi-resolution segmentation for
357 automatic habitat boundary delineation, (ii) the GLCM texture definition, and (iii) temporal
358 mapping (Tables 3, 4).

359

360

4.3 Accuracy Assessment

Two confusion matrices of the habitat classification maps, with nine classes, for the years 2001 and 2014 are presented in Tables 4 and Table 5. Overall mapping accuracies and kappa coefficients respectively for both years were above 92 % and 0.91. A moderate level of confusion occurred between shrubland and open shrubland, and this confusion occurred for several reasons. The change from open shrubland to shrubland is a natural continuum and boundaries between them are typically gradual and diffuse, thus a subjective decision is required to establish the boundary. The subjectivity was accommodated by considering the object-based image paradigm. However, open shrubland differs from shrubland by having a lower density of woody vegetation and generally having more open canopy. Similarly, a certain amount of confusion could arise between young emerging forest and shrubland due to insignificant differences in the structure of tree crowns and shadows. The decision whether an object is in one class or another can be based on small density differences and structural changes, which in turn generates classification inaccuracies

Table 4 Confusion matrix generated for accuracy assessment of habitat map of 2001

		Predicted Habitat Information										
		F	OF	SH	SG	GL	BA	BU	W	PF	Sum	User's Accuracy (%)
Ground Reference Information	F	57	0	0	0	0	0	0	0	1	58	98.3
	OF	0	9	0	0	0	0	0	0	0	9	100.0
	SH	4	0	25	2	0	0	0	0	0	31	80.7
	SG	1	0	1	25	2	0	0	0	0	29	86.2
	GL	0	0	3	7	101	0	0	0	0	111	90.9
	BA	0	0	0	0	2	18	0	0	0	20	90.0
	BU	0	0	0	0	0	1	15	0	0	16	93.8
	W	0	0	0	0	0	0	0	20	0	20	100.0
	PF	2	0		0	0	0	0	0	47	49	95.9
	Sum	64	9	29	34	105	19	15	20	48		
Producer's Accuracy (%)		89.1	100.0	86.2	73.5	96.2	94.7	100.0	100.0	97.9		

Total Samples = 343 Correct Samples = 317 Overall Accuracy = 92.42 % Kappa Coefficient = 0.91

Table 5 Confusion matrix generated for accuracy assessment of habitat map of 2014

		Predicted Habitat Information										
		F	OF	SH	SG	GL	BA	BU	W	PF	Sum	User's Accuracy (%)
Ground Reference Information	F	63	0	0	0	0	0	0	0	1	64	98.44
	OF	0	15	0	0	0	0	0	0	0	15	100.00
	SH	1	1	51	3	0	0	0	0	0	56	91.07
	SG	0	1	1	39	1	0	0	0	0	42	92.86
	GL	0	0	1	2	70	0	0	0	0	73	95.89
	BA	0	0	0	0	0	18	1	0	0	19	94.74
	BU	0	0	0	0	0	1	8	0	0	9	88.89
	W	0	0	0	0	0	0	0	20	0	20	100.00
	PF	2	0	0	0	0	0	0	0	55	57	96.49
	Sum	66	17	53	44	71	19	9	20	56		
Producer's Accuracy (%)		95.5	88.2	96.2	88.6	98.6	94.7	88.9	100.0	98.2		

Total Samples = 342 Correct Samples = 321 Overall Accuracy = 95.49 % Kappa Coefficient = 0.95

4.4 Landscape composition over time

Analysis of the sequential habitat maps shows that the landscape has progressively transformed from a grassland-dominated to a forest-dominated landscape over the 70 years of succession. Forest cover has increased over time from 0.17 % of the landscape (4.82 ha) in 1945 to 36.50 % (1019.23 ha) in 2014 at an average annual rate of increase of 7.76 % over the 70-year study period (Figure 4, Table 6). Forest progressed from isolated patches of shrub in valley bottoms (Figure 5), to solid patches of shrubland infilling across interfluves, followed by advance a broader front later, and at higher elevations. By 2014 the landscape had gradually consolidated as patches of successional stages became connected and larger in size, recognized by OBIA at higher object levels, as segments with larger scale factor and higher heterogeneity.

390

391 **Table 6** Area of habitat classes and annual rate of change over the time periods

Habitat Classes	Area in hectare					Annual rate change (%)				
	1945	1963	1989	2001	2014	1945-1963	1963-1989	1989-2001	2001-2014	1945-2014
F	4.82	19.85	140.03	579.04	1019.23	7.86	7.51	10.92	4.71	7.76
OF	0.22	27.69	38.09	108.32	27.54	26.91	1.23	8.04	-11.41	7.01
SH	24.03	175.05	464.18	418.70	650.43	11.03	3.75	-0.79	3.67	4.78
OS	170.99	203.57	245.27	261.49	421.29	0.97	0.72	0.49	3.97	1.31
GL	2203.17	1805.62	1479.82	969.92	219.92	-1.11	-0.77	-3.25	-12.37	-3.34
BA	336.95	71.76	52.57	52.16	51.23	-8.59	-1.20	-0.06	-0.15	-2.73
BU	0.41	5.21	8.80	12.51	12.51	14.17	2.02	2.70	0.00	4.97
W	57.21	57.21	57.21	57.21	57.21	0.00	0.00	0.00	0.00	0.00
PF	0.00	431.85	311.20	337.81	337.81	0.00	-1.26	0.63	0.00	0.00

392

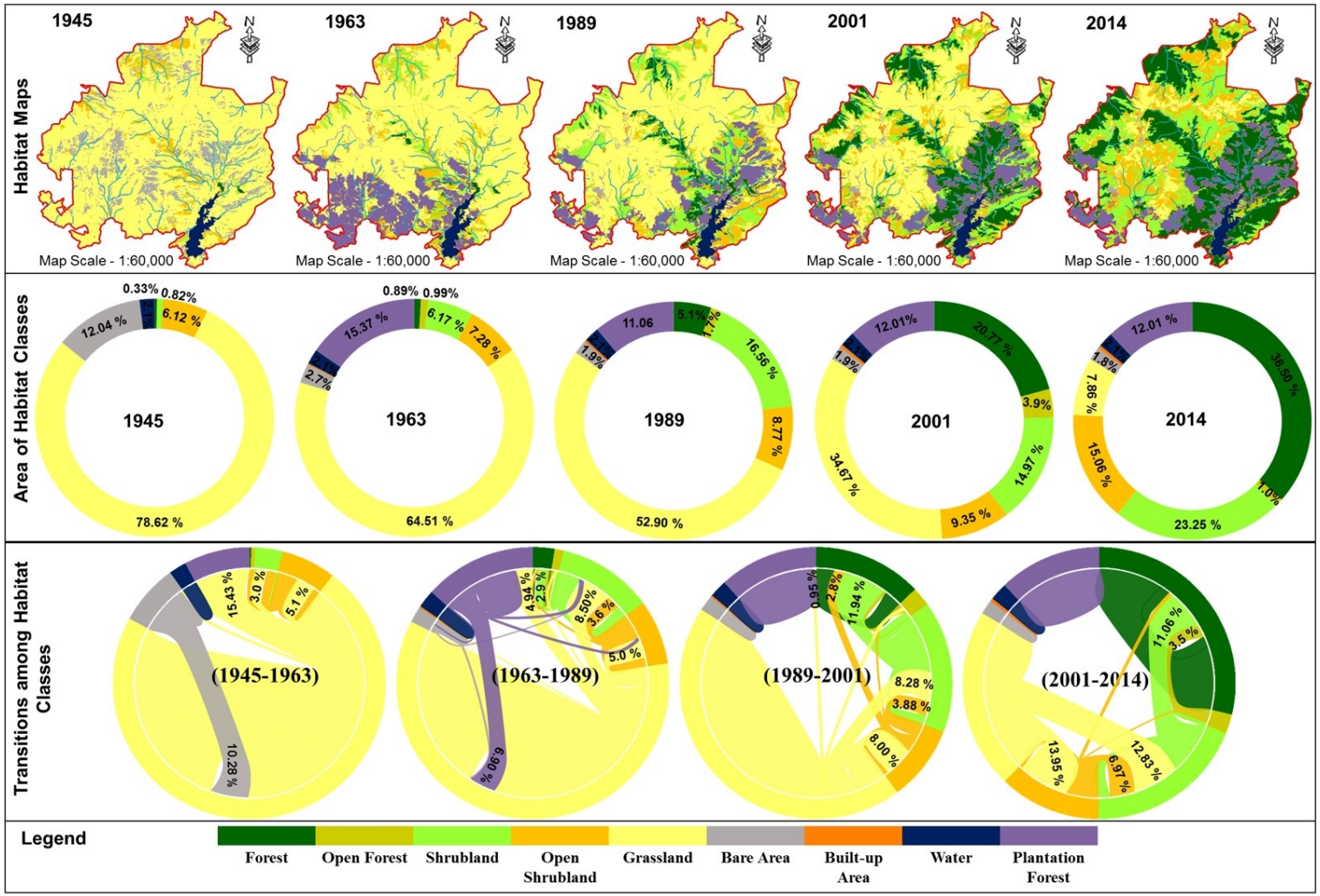

393

394 **Figure 4** Maps indicate spatial patterns of habitat classes and the doughnut graphs show proportions of each class in 1945, 1963,
395 1989, 2001, 2014, while the chord diagrams indicate major transitions among the habitat classes for each of the sequentially paired
396 successive time periods (1945 -1963, 1963 – 1989, 1989 – 2001, 2001 – 2014) which is based on the gains and losses determined from
397 transition matrices by using equations IV-VIII.

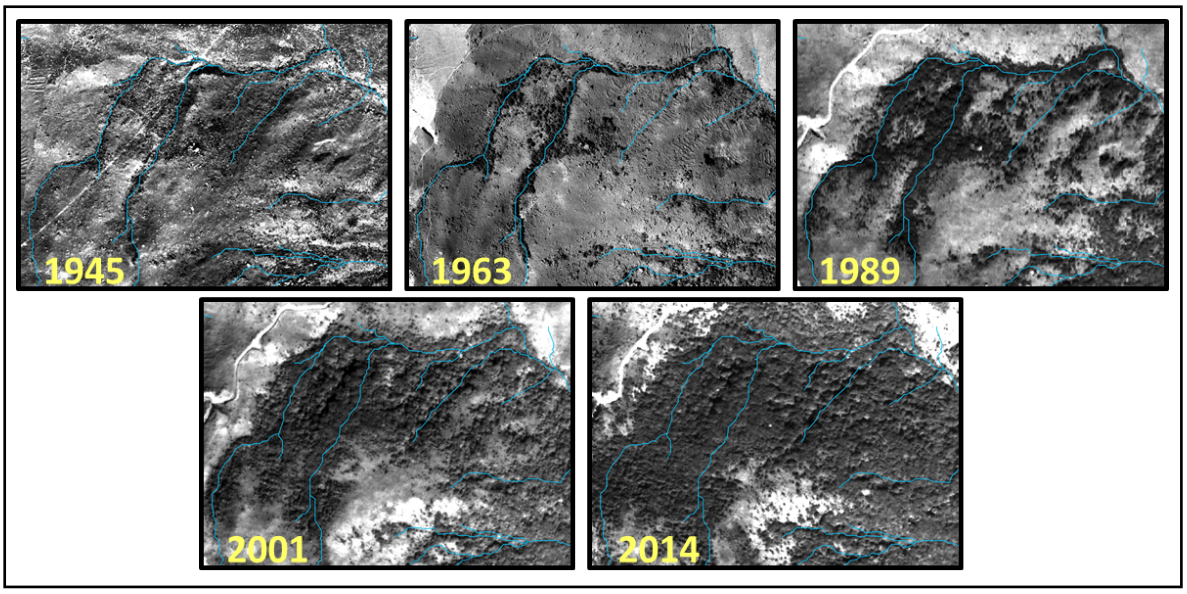

Figure 5: Image sequence showing natural forest regeneration starting from shrub colonization in valley bottoms which then expanded spatially by infilling across interfluves.

5. Discussion

A semi-automated multiscale object-based approach was applied to a set of aerial photographs and high-resolution satellite images to map structural changes in natural vegetation over the last 70 years, from 1945 to 2014. The segmentation process permitted automated digitizing of habitat boundaries, which is a more computer-oriented method than the manual digitizing normally used for single channel remote sensing data. The image objects delineated through multiscale segmentation combine textural and tonal characteristics of image object primitives which represented the structural characteristics of vegetation classes. It is important to understand that a fully automatic approach to habitat classification is not easy in a complex tropical forest ecosystem especially when using black and white aerial photographs of different qualities and scales. In this study, OBIA was able to automatically delineate habitat boundaries using the same objective criteria for both black and white aerial photos and satellite images, based on knowledge-based thresholds of GLCM texture features. This permitted object-oriented and consistent temporal change mapping. The combination of these approaches is so far little explored for mapping forest succession despite the widespread use of OBIA methods in a variety of remote sensing studies for forest inventories (Blaschke, 2010). Image objects produced from image segmentation are readily available in vector format which can be directly imported and analyzed in a vector-based GIS software (e.g. ArcGIS, QGIS). This is more convenient and cost-effective than the traditional approach of manual digitization of habitat boundaries from black and white aerial photos and satellite images (Figure 2 – g, h, i).

Many studies have demonstrated the multi-scale object-based approach for precise delineation of forest vegetation boundaries in natural landscapes from high resolution satellite images or from aerial photographs (Gergel et al., 2007; Hay et al., 2005; Johansen et al., 2007; Mallinis et al., 2008; Nichol and Wong, 2008; Radoux et al., 2011). Although some studies represent the promising results obtained from object-based image analysis for detailed habitat mapping

427 with very high-resolution satellite imagery, most have not achieved above 80 % overall
428 accuracy. This is due to the natural confusion among different structural classes of vegetation
429 which are difficult to separate, even when using single-date remote sensing imagery. This
430 study, however, has achieved significantly higher overall accuracies, of over 92 % by
431 combining OBIA and multi-temporal mapping. The approach adopted in this study also
432 demonstrates the importance of object-based delineation of habitat patches to overcome the
433 modifiable areal unit problem (MAUP) (Marceau et al., 1994) which results from the use of
434 different quality and scale of remote sensing images.

435 The ability to define the transitional classes 'Open Shrubland', 'Shrubland' and "Open Forest'
436 objectively as multi-scale objects by their definable and consistent tone and texture provided
437 meaningful maps, which have not been previously available for studying long-term forest
438 succession. These are transitional classes in the succession, differing only by the proportion of
439 woody vegetation within a grassland matrix. The proportion is significant as the spacing
440 between woody patches governs the dispersal ability of forest seed dispersal agents, mainly
441 birds, and succession may be impeded if distances are beyond the dispersal distance (Weir and
442 Corlett, 2006). Forest managers may use the implied 'objective' measures of shrub density to
443 assist succession by these natural dispersal agents, by planting in areas with slow progression
444 to forest. The ability to distinguish natural forest from plantations was assisted by the
445 multitemporal analysis, as the regular pattern of plantations in early growth stages persisted
446 over time within the original plantation boundaries, in spite of their visual similarity to forest
447 as they matured.

448 This high rate of forest regeneration observed is surprising, and provides new empirical
449 evidence to forest managers that expensive forest plantation policies are unnecessary if fire is
450 controlled. Until now, such evidence has not been available due to the difficulty of identifying

and following forest succession with consistent and accurate structural definition of forest classes over a long period.

As forest is the climax vegetation of Hong Kong, the inevitable decline in habitat diversity observed in this study, as succession proceeds to closed forest, may be viewed as a natural and desirable first step in the restoration of the ecosystem. Although the secondary forest has attained a species richness comparable to or greater than the old growth forest sites, their composition is very different from the old growth forest stands in the study area. Furthermore, the absence of specialist forest fauna may be an issue in the future structure of this regenerated landscape, especially since the shade-tolerant, later successional forest species have poor dispersal abilities. Therefore, to manage natural succession and to guarantee enough genetic diversity in Hong Kong's newly establishing forests, climax trees may be planted strategically in carefully selected plots where the oldest forest pioneers are established. In this regard, time-consistent mapping forest habitat patches different age group resulting in this multi-sensor and muti-temporal habitat mapping paradigm will play a pivotal role in devising effective policies for low-cost management of regenerating forests.

In this study, sequential analysis of time series remote sensing data permitted mapping of forest patches at several successional stages, which enabled chronosequence analysis of floristic traits and successional trajectories of the recovering forest. Furthermore, composite maps of forest cover patches with different successional stages can also help for site-specific management of the recovering forest, for example, introduction of late successional tree species where forest pioneers have been established.

6. Conclusion

The Modifiable Areal Unit Problem is inevitable when historic aerial photographs are combined with recent high-resolution satellite images to monitor change over time scales earlier than the operational use of satellite platforms. The multi-scale and contextual approach inherent in OBIA can be applied to monitor secondary vegetation succession by defining fragmented and regenerating habitat patches as consistent and comparable image objects (areal units) across multiple datasets. The resulting ability to observe real changes in these objects over time permits an understanding of spatial and temporal patterns and processes of vegetation structure. In addition to fine-scale mapping of vegetation structure, the multi-temporal OBIA approach identifies forest patches of different age groups (e.g., old growth forest, medium aged forest and young forest). This provides forest managers with powerful information to understand processes of natural regeneration of forests in degraded landscapes. In addition, it allows for informed intervention in the succession, in situations where progression is deemed too slow, i.e. the observed rate of progression of woody vegetation invading grassland, i.e. the 'Open Shrubland' category succeeding to 'Closed Shrubland' then 'Open Forest' to 'Forest'. Restoration of landscapes degraded by decades of shifting cultivation, which are common in sub-tropical Asia, is becoming more desirable as rural population densities exceed those which shifting cultivation can support (Bhatt et al., 2010; Karthik and Veeraswami, 2009), and as governments participate in carbon sequestration and biodiversity conservation projects (Chazdon et al., 2016). The semi-automatic approach described in this study resulted in a precise classification of high resolution panchromatic (single channel) aerial photographs, with overall mapping accuracies above 92 %. This improvement in habitat delineation and classification of habitat patches by the object-based, the multi-temporal approach was able to provide new, science-based understanding of the processes of forest regeneration as inputs to forest management and landscape rehabilitation policies. Furthermore, this multi-temporal object bases paradigm of mapping forest habitat patches of different age groups can play a vital role in enhancing models to estimate accumulation of aboveground biomass in regenerating tropical forest (Chazdon et al., 2016). This can help in site-specific implementation of REDD-plus (Reduced Emissions from Deforestation and forest Degradation) for devising effective policies for management, conservation, and enhancement of carbon stocks of regenerating tropical secondary forest.

Acknowledgements

The work has been supported by the Hong Kong PhD Fellowship Program and a research grant from the Hong Kong Polytechnic University, grant No. 1-ZE24, and a grant PolyU 1-BBWD from the Research Institute for Sustainable Urban Development, the Hong Kong Polytechnic University. Authors would also like to acknowledge the support drawn of Agriculture, Fisheries and Conservation Department (AFCD), and the Lands Department of Hong Kong.

513 **References:**

514 Allard, A., 2003. Vegetation changes in mountainous area - a monitoring methodology based
515 on aerial photographs, high-resolution satellite images, and field investigation.
516 Stockholm University.

517 Bhatt, B.P., Singha, L.B., Satapathy, K.K., Sharma, Y.P., Bujarbaruah, K.M., 2010.
518 Rehabilitation of shifting cultivationareas through agroforestry: A case study in Eastern
519 Himalaya, IndiaIA. J. Trop. For. Sci. 22, 13–20.

520 Blaschke, T., 2010. Object based image analysis for remote sensing. ISPRS J. Photogramm.
521 Remote Sens. 65, 2–16. doi:10.1016/j.isprsjprs.2009.06.004

522 Cao, H., Wu, L., Wang, Z., Huang, Z., Li, L., Wei, S., Lian, J., Ye, W., 2013. Dinghushan
523 Lower Subtropical Forest Dynamics Plot: Tree Species and Their Distribution Patterns.
524 China Forestry Press, Beijing.

525 Chazdon, R.L., Broadbent, E.N., Rozendaal, D.M.A., Bongers, F., Zambrano, A.M.A., Aide,
526 T.M., Balvanera, P., Becknell, J.M., Boukili, V., Brancalion, P.H.S., Craven, D.,
527 Almeida-Cortez, J.S., Cabral, G.A.L., de Jong, B., Denslow, J.S., Dent, D.H., DeWalt,
528 S.J., Dupuy, J.M., Durán, S.M., Espírito-Santo, M.M., Fandino, M.C., César, R.G., Hall,
529 J.S., Hernández-Stefanoni, J.L., Jakovac, C.C., Junqueira, A.B., Kennard, D., Letcher,
530 S.G., Lohbeck, M., Martínez-Ramos, M., Massoca, P., Meave, J.A., Mesquita, R., Mora,
531 F., Muñoz, R., Muscarella, R., Nunes, Y.R.F., Ochoa-Gaona, S., Orihuela-Belmonte, E.,
532 Peña-Claros, M., Pérez-García, E.A., Piotto, D., Powers, J.S., Rodríguez-Velazquez, J.,
533 Romero-Pérez, I.E., Ruíz, J., Saldarriaga, J.G., Sanchez-Azofeifa, A., Schwartz, N.B.,
534 Steininger, M.K., Swenson, N.G., Uriarte, M., van Breugel, M., van der Wal, H.,
535 Veloso, M.D.M., Vester, H., Vieira, I.C.G., Bentos, T.V., Williamson, G.B., Poorter, L.,
536 2016. Carbon sequestration potential of second-growth forest regeneration in the Latin
537 American tropics. Sci. Adv. 2, e1501639. doi:10.1126/sciadv.1501639

538 Congalton, R., Gu, J., Yadav, K., Thenkabail, P., Ozdogan, M., 2014. Global Land Cover
539 Mapping: A Review and Uncertainty Analysis. Remote Sens. 6, 12070–12093.
540 doi:10.3390/rs61212070

541 Delang, C.O., Hang, Y.Y., 2009. Remote Sensing-Based Estimation of Carbon Sequestration
542 in Hong Kong Country Parks from 1978 to 2004. Open Environ. Sci. 3, 97–115.

543 Dissanska, M., Bernier, M., Payette, S., 2009. Object-based classification of very high
544 resolution panchromatic images for evaluating recent change in the structure of
545 patterned peatlands. Can. J. Remote Sens. 35, 189–215. doi:10.5589/m09-002

546 Dudgeon, D., Corlett, R., 2011. The Ecology and Biodiversity of Hong Kong (revised ed.).
547 Hong Kong: Cosmos Books & Lions Nature Education Foundation.

548 Etter, A., McAlpine, C., Pullar, D., Possingham, H., 2005. Modeling the age of tropical moist
549 forest fragments in heavily-cleared lowland landscapes of Colombia. For. Ecol. Manage.
550 208, 249–260. doi:10.1016/j.foreco.2004.12.008

551 Faber-Langendoen, D., 1992. Ecological constraints on rain forest management at Bajo
552 Calima, western Colombia. For. Ecol. Manage. 53, 213–244. doi:10.1016/0378-
553 1127(92)90044-A

554 Flanders, D., Hall-Beyer, M., Pereverzoff, J., 2003. Preliminary evaluation of eCognition

555 object-based software for cut block delineation and feature extraction. Can. J. Remote
556 Sens. 29, 441–452. doi:10.5589/m03-006

557 Galo, A.J.J., 2016. Acquisition, Characteristics and Preprocessing of Passive Remote Sensing
558 Images in Tropical Forestry, in: Pancel, L., Köhl, M. (Eds.), Tropical Forestry
559 Handbook. Springer Berlin Heidelberg, Berlin, Heidelberg, Heidelberg, pp. 1–30.
560 doi:10.1007/978-3-642-41554-8_108-2

561 Gergel, S.E., Stange, Y., Coops, N.C., Johansen, K., Kirby, K.R., 2007. What is the Value of
562 a Good Map? An Example Using High Spatial Resolution Imagery to Aid Riparian
563 Restoration. Ecosystems 10, 688–702.

564 Geri, F., Rocchini, D., Chiarucci, A., 2010. Landscape metrics and topographical
565 determinants of large-scale forest dynamics in a Mediterranean landscape. Landsc.
566 Urban Plan. 95, 46–53. doi:10.1016/j.landurbplan.2009.12.001

567 Grainger, A., 1988. Estimating Areas of Degraded Tropical Lands Requiring Replenishment
568 of Forest Cover. Int. Tree Crop. J. 5, 31–61. doi:10.1080/01435698.1988.9752837

569 Guevara, S., Laborde, J., 1993. Monitoring seed dispersal at isolated standing trees in tropical
570 pastures: consequences for local species availability. Vegetatio 107, 319–338.
571 doi:10.1007/BF00052232

572 Hall-Beyer, M., 2007. GLCM texture: an online tutorial. Version 2.10 February 2007 [WWW
573 Document]. URL http://www.fp.ucalgary.ca/mhallbey/tutorial.htm (accessed 8.12.14).

574 Haralick, R.M., Shanmugam, K., Dinstein, I., 1973. Textural Features for Image
575 Classification. IEEE Trans. Syst. Man. Cybern. 3, 610–621.
576 doi:10.1109/TSMC.1973.4309314

577 Hartshorn, G.S., 1980. Neotropical Forest Dynamics. Biotropica 12, 23. doi:10.2307/2388152

578 Hay, G.J., Castilla, G., Wulder, M. a., Ruiz, J.R., 2005. An automated object-based approach
579 for the multiscale image segmentation of forest scenes. Int. J. Appl. Earth Obs. Geoinf.
580 7, 339–359. doi:10.1016/j.jag.2005.06.005

581 Helmer, E.H., 2000. The landscape ecology of tropical secondary forest in montane Costa
582 Rica. Ecosystems 3, 98–114. doi:10.1007/s100210000013

583 HK-Landsd, 2014. Lands Department: The Government of the Hong Kong Special
584 Administrative Region [WWW Document]. URL
585 http://www.landsd.gov.hk/en/about/welcome.htm

586 Jingyun, F., Yide, L., Biao, Z., Guohua, L., Guangyi, Z., 2004. Community structures and
587 species richness is the montane rain forest of Jianfengling,Hainan island,China.
588 Biodivers. Sci.

589 Johansen, K., Coops, N.C., Gergel, S.E., Stange, Y., 2007. Application of high spatial
590 resolution satellite imagery for riparian and forest ecosystem classification. Remote
591 Sens. Environ. 110, 29–44. doi:10.1016/j.rse.2007.02.014

592 Karthik, T., Veeraswami, G.G., 2009. Review article Forest recovery following shifting
593 cultivation : an overview of existing research. Trop. Conserv. Sci. 2, 374–387.

594 Kim, D., Sexton, J.O., Townshend, J.R., 2015. Accelerated deforestation in the humid tropics
595 from the 1990s to the 2000s. Geophys. Res. Lett. 42, 1–7.

596 doi:10.1002/2014GL062777.Received

597 Leung, G.P.C., Hau, B.C.H., Corlett, R.T., 2008. Exotic plant invasion in the highly degraded
598 upland landscape of Hong Kong, China. Biodivers. Conserv. 18, 191–202.
599 doi:10.1007/s10531-008-9466-5

600 Lucas, R.M., Honzák, M., do Amaral, I., Curran, P.J., Foody, G.M., 2002. Forest
601 regeneration on abandoned clearances in central Amazonia 37–41.
602 doi:10.1080/01431160110069791

603 Mallinis, G., Koutsias, N., Tsakiri-Strati, M., Karteris, M., 2008. Object-based classification
604 using Quickbird imagery for delineating forest vegetation polygons in a Mediterranean
605 test site. ISPRS J. Photogramm. Remote Sens. 63, 237–250.
606 doi:10.1016/j.isprsjprs.2007.08.007

607 Marceau, D.J., Gratton, D.J., Fournier, R.A., Fortin, J.P., 1994. Remote sensing and the
608 measurement of geographical entities in a forested environment. 2.The optimal spatial
609 resolution. Remote Sens. Environ. 49, 105–117. doi:10.1016/0034-4257(94)90047-7

610 Mathieu, R., Aryal, J., Chong, A.K., 2007. Object-Based Classification of Ikonos Imagery for
611 Mapping Large-Scale Vegetation Communities in Urban Areas. Sensors 7, 2860–2880.
612 doi:10.3390/s7112860

613 Munsi, M., Malaviya, S., Oinam, G., Joshi, P.K., 2010. A landscape approach for quantifying
614 land-use and land-cover change (1976-2006) in middle Himalaya. Reg. Environ. Chang.
615 10, 145–155. doi:10.1007/s10113-009-0101-0

616 Nichol, J., Wong, M.S., 2008. Habitat Mapping in Rugged Terrain Using Multispectral
617 Ikonos Images. Photogramm. Eng. Remote Sens. 74, 1325–1334.
618 doi:10.14358/PERS.74.11.1325

619 Pellerin, S., Lavoie, C., 2003. Reconstructing the recent dynamics of mires using a
620 multitechnique approach. J. Ecol. 91, 1008–1021. doi:10.1046/j.1365-
621 2745.2003.00834.x

622 Perz, S., Skole, D., 2003. Secondary forest expansion in the Brazilian Amazon and the
623 refinement of forest transition theory. Soc. Nat. Resour. 16, 277–294.
624 doi:10.1080/08941920390178856

625 Pontius, R.G., Shusas, E., McEachern, M., 2004. Detecting important categorical land
626 changes while accounting for persistence. Agric. Ecosyst. Environ. 101, 251–268.
627 doi:10.1016/j.agee.2003.09.008

628 Pringle, R.M., Syfert, M., Webb, J.K., Shine, R., 2009. Quantifying historical changes in
629 habitat availability for endangered species: Use of pixel- and object-based remote
630 sensing. J. Appl. Ecol. 46, 544–553. doi:10.1111/j.1365-2664.2009.01637.x

631 Puyravaud, J.-P., 2003. Standardizing the calculation of the annual rate of deforestation. For.
632 Ecol. Manage. 177, 593–596. doi:10.1016/S0378-1127(02)00335-3

633 Qi, X., Wang, K., Zhang, C., 2013. Effectiveness of ecological restoration projects in a karst
634 region of southwest China assessed using vegetation succession mapping. Ecol. Eng. 54,
635 245–253. doi:10.1016/j.ecoleng.2013.01.002

636 Rabia, A.H., Terribile, F., 2013. Semi-Automated Classification of Gray Scale Aerial
637 Photographs using Geographic Object Based Image Analysis (GEOBIA) Technique.

638 Geophys. Res. Abstr. 15, 2013.

639 Radoux, J., Bogaert, P., Fasbender, D., Defourny, P., 2011. Thematic accuracy assessment of
640 geographic object-based image classification. Int. J. Geogr. Inf. Sci. 25, 895–911.
641 doi:10.1080/13658816.2010.498378

642 Saldarriaga, J.G., West, D.C., Tharpt, M.L., Uhq, C., Tharp, M.L., Uhl, C., Tharpt, M.L.,
643 Uhq, C., Tharp, M.L., Uhl, C., 1988. Long-Term Chronosequence of Forest Succession
644 in the Upper Rio Negro of Colombia and Venezuela. J. Ecol. 76, 938–958.
645 doi:10.2307/2260625

646 Sann, B., Kanzaki, M., Ohta, S., 2016. Vegetation patterns and species-filtering effects of soil
647 in secondary succession in a tropical dry forest in central Myanmar. J. Trop. Ecol. 32,
648 116–124. doi:10.1017/S026646741600002X

649 Sarker, M.L.R., 2010. Estimation of forest biomass using remote sensing. Hong Kong : Dept.
650 of Land Surveying and Geo-Informatics, The Hong Kong Polytechnic University, 2010.,
651 Hong Kong.

652 Sodhi, N.S., Brook, B.W., 2008. Fragile Southeast Asian biotas. Biol. Conserv. 141, 883–
653 884. doi:10.1016/j.biocon.2007.12.027

654 Song, C., Woodcock, C.E., 2002. The spatial manifestation of forest succession in optical
655 imagery The potential of multiresolution imagery 82, 271–284.

656 Teferi, E., Bewket, W., Uhlenbrook, S., Wenninger, J., 2013. Understanding recent land use
657 and land cover dynamics in the source region of the Upper Blue Nile, Ethiopia: Spatially
658 explicit statistical modeling of systematic transitions. Agric. Ecosyst. Environ. 165, 98–
659 117. doi:10.1016/j.agee.2012.11.007

660 Turner, I.M., Corlett, R.T., 1996. The conservation value of small, isolated fragments of
661 lowland tropical rain forest. TREE 11, 330–333.

662 Turner, I.M., Wong, Y.K., Chew, P.T., Ibrahim, bin A., 1997. Tree species richness in
663 primary and old secondary tropical forest in Singapore. Biodivers. Conserv. 6, 537–543.
664 doi:10.1023/A:1018381111842

665 Turner, I.M., Wong, Y.K., Chew, P.T., Ibrahim, A. Bin, 1996. Rapid assessment of tropical
666 rain forest successional status using aerial photographs. Biol. Conserv. 77, 177–183.
667 doi:10.1016/0006-3207(95)00145-X

668 Vogeler, J., Braaten, J., Slesak, R., Falkowski, M., 2018. Extracting the full value of the
669 Landsat archive: Inter-sensor harmonization for the mapping of Minnesota forest canopy
670 cover (1973–2015). Rev. 209, 363–374. doi:10.1016/j.rse.2018.02.046

671 Zhuang, X., Corlett, R.T., 1997. Forest and forest succession in Hong Kong, China. J. Trop.
672 Ecol. 14, 857–866.

673